Available online at www.sciencedirect.com

SciVerse ScienceDirect

Ceramics International 38 (2012) 1507–1513

CERAMICS INTERNATIONAL

www.elsevier.com/locate/ceramint

# Influence of Ni and Co doping on the stability of the $ErMnO_3$ perovskites processed by mechanochemical synthesis

A. Moure [a,*], T. Hungría [b], A. Castro [b], J. Galy [c], O. Peña [d], I. Martínez [b], J. Tartaj [a], C. Moure [a]

[a] Instituto de Cerámica y Vidrio, CSIC, C/Kelsen, 5, 28049 Madrid, Spain

[b] Instituto de Ciencia de Materiales de Madrid, CSIC, c/Sor Juana Inés de la Cruz, 3 Cantoblanco, 28049 Madrid, Spain

[c] Centre d'Elaboration de Matériaux et d'Etudes Structurales, CNRS, 29, rue Jeanne Marvig, 31055 Toulouse, France

[d] Sciences Chimiques de Rennes, UMR 6226, Université de Rennes 1, Rennes, France

Received 19 July 2011; received in revised form 15 September 2011; accepted 15 September 2011

Available online 21 September 2011

**Abstract**

Mechanosynthesis in tungsten carbide vessels and planetary mill is an effective method to prepare materials with $ErMnO_3$ derived compositions and perovskite-type structure. In this work, the effect of the doping with low contents of Co and Ni cations on the stability of such oxides is studied. The obtained perovskites are highly distorted for all compositions. The transition to the more stable hexagonal phase occurs at lower temperatures for Co-doped materials, due to the presence of $Co^{3+}$ cations that do not involve any change of oxidation state for $Mn^{3+}$ Jahn–Teller cations. Spark Plasma Sintering (SPS) was carried out at 900 °C or 950 °C and 120 MPa to obtain dense ceramics, keeping the perovskite-type structures. The magnetic properties of the obtained materials are also shown.



*Keywords:* Magnetic materials; Nanostructures; Ceramics

## 1. Introduction

Rare earth manganites with perovskite structure $REMnO_3$ have attracted much interest during last years due to their different and interesting properties, as the colossal magnetoresistance observed in hole-doped $LaMnO_3$ [1], the multiferroicity of the compositions with larger ionic radii, as $TbMnO_3$ [2], or more recently, for the ones with the smallest ionic radius, as $HoMnO_3$, $YMnO_3$ or $ErMnO_3$ [3,4] when they present an orthorhombic perovskite-type structure. For these last series of compositions for RE = Ho, . . ., Lu, (and also for Y and Sc), there is a practical limitation in their processing. At difference of the ternary oxides $REFeO_3$, crystallizing with an orthorhombic perovskite-type structure [5] (Space Group Pbnm), hereafter designed by OP, these manganese ternary oxides with smaller ionic radii crystallize in the hexagonal system (HS), with S.G. $P6_3cm$. This fact occurs despite the practically same ionic radius corresponding to $Fe^{3+}$ and $Mn^{3+}$ [6] and, therefore, having the same tolerance factor, $t$, for the perovskite-type structure, defined as:

$$t = \frac{r_A + r_O}{\sqrt{2}(r_B + r_O)} \quad (1)$$

where $r_A$ and $r_B$ are the ionic radii of the A and B cation, respectively, and $r_O$ is that of the $O^{2-}$ anion.

The reason for the instability of the OP structure and therefore the formation of the hexagonal phase is the Jahn–Teller nature of the $Mn^{3+}$ cation. Due to the strong Hund's rule coupling, the manganese ions adopt a high spin configuration $t_{2g}^3 e_g^1$. According to Jahn–Teller (JT) theorem, a distortion of the local octahedral environment, removing the degeneracy of the $e_g$ orbitals, is energetically favorable. This distortion is accomplished by lengthening two of the Mn–O trans bond, which lowers the energy of the occupied $3d_z^2$ orbitals with respect to the empty $3d_{x^2-y^2}^2$ orbitals. The filled $3d_z^2$ orbitals form a zigzag pattern in the $xy$ plane which leads to an expansion of the $a$ and $b$ unit cell dimensions [7,8]. This cooperative effect together with tolerance factor lowering explains the formation of HS for the small rare-earth cation compounds [9]. Superexchange interactions between $Mn^{3+}$ cations stabilize an A-type antiferromagnetic spin arrangement

* Corresponding author.
*E-mail address:* alberto.moure@icv.csic.es (A. Moure).

0272-8842/$36.00 
doi:10.1016/j.ceramint.2011.09.034

(ferromagnetic layers coupled antiferromagnetically to each other), with a semiconducting or isolating behavior [10–12].

The suppression of this cooperative effect leads to the transition from HS → OP [13–16], which can also be induced by the formation of solid solutions (RE,Me)$MnO_3$, Me = Ca, Sr, Ba, and other divalent cations, with the formation of $Mn^{4+}$ cations at the expenses of $Mn^{3+}$ ones [10,17–19]. Phases RE(Mn,M)$O_3$, M = $Ni^{2+}$, $Co^{2+}$, $Cu^{2+}$ show the same effect by the substitution of non-JT cations for $Mn^{3+}$ and the corresponding oxidation of manganese cations to $Mn^{4+}$ [10,20].

The more usual procedure to obtain $REMnO_3$ OP-type compounds for RE = Er, . . ., Y, is the synthesis of the hexagonal phase by solid-state reaction between oxides or by an alternative chemical route, as powder or as solid body, lately subjected to very high pressures, as large as 5 GPa or higher, and at relatively high temperatures, 1100–1300 °C [11,12,21,22]. Recently, the authors have reported an alternative method to process $ErMn_{1-x}Ni_xO_3$ ($x$ = 0, 0.1), ceramic materials with perovskite structure by mechanosynthesis after 24 h of milling in tungsten carbide media from an oxide mixture [23]. The perovskite structure is stable up to 900–1000 °C, before transition to a hexagonal structure. The transition temperature was found to be higher in the Ni-doped material with regard to pure $ErMnO_3$. Dense ceramics with such structure could only be obtained by SPS at $T < 1000$ °C. These results open the possibility of processing perovskite $REMnO_3$ materials with RE = Er, . . ., Lu and Y with small ionic radius. In addition, it is expected that the formation of solid solutions by mechanosynthesis, with small doping quantities of different cations could influence the stability and properties of these phases.

In this work, solid solutions of $ErMn_{1-x}Ni_xO_3$ and $ErMn_{1-x}Co_xO_3$ ($x$ = 0.05 and 0.15) with perovskite-type structure were synthesized by mechanosynthesis. The influence of the doping type (Co or Ni) on the stability of the perovskite phases is studied in terms of the Jahn–Teller effect. Ceramics were consolidated by Spark Plasma Sintering (SPS) at moderate temperatures (<1000 °C), and highly dense nanostructured ceramics were also achieved. Magnetic features are reported and compared with other rare-earth manganites with orthorhombic perovskite structures.

## 2. Experimental

Powders of perovskite-type $ErMn_{1-x}Ni_xO_3$ and $ErMn_{1-x}Co_xO_3$ phases, $x$ = 0.05, 0.15, were obtained by high energy ball milling. The stoichiometric quantities of $Er_2O_3$, $Mn_2O_3$, NiO and $Co_3O_4$ necessary to obtain 10 g of the wanted compositions were placed in a tungsten carbide (WC) vessel (volume 250 ml) with seven also WC balls, 2 cm diameter (ball/powder weight ratio ∼45/1). Mechanosynthesis was carried out with a Fritsch Pulverisette 6 planetary mill, operating at 300 rpm.

Evolution with different milling times of the precursors was monitored by Bragg–Brentano X-ray diffraction (XRD) with a Brüker AXS D8 Advance diffractometer. Cu $K_\alpha$ radiation ($\lambda$ = 1.5418 Å) and a $5 \times 10^{-2}$ deg ($2\theta$) $s^{-1}$ scan rate were used. Milled materials were uniaxially pressed into pellets and treated at temperatures between 880 and 1030 °C and later characterized by XRD. The phases were identified using a scanning rate of typically $3.3 \times 10^{-2}$ deg ($2\theta$) $s^{-1}$.

Ceramics keeping the perovskite structure were processed by Spark Plasma Sintering using a SPS 2080 Sumitomo apparatus. A cylindrical graphite die (8 mm inner diameter) was filled with the powder and a pulsed direct current was passed through the die while an increasing uniaxial pressure was applied (up to 120 MPa). The sample was heated to the final temperature (900–950 °C) at heating rates of 180–190 °C $min^{-1}$. The final sintering temperature and 120 MPa pressure were maintained for 1 min.

The microstructure of the obtained ceramics was characterized by transmission electron microscopy, TEM, which was carried out in a JEOL 2100 FEG working at 200 kV.

Magnetic measurements were performed on a Quantum Design MPMS-XL5 SQUID (superconducting quantum interference device) magnetometer between 2 and 300 K, under different applied fields (10 kOe for measurements in the paramagnetic state and 100 Oe for ZFC/FC cycles); magnetization $M(H)$ was recorded up to $H$ = 50 kOe at $T$ = 2 K, with increasing and decreasing fields.

## 3. Results and discussion

Fig. 1 shows the evolution with milling time from the initial oxide mixture, for both Ni and Co doped compositions. Only the XRD patterns belonging to the sample with $x$ = 0.05 are shown, but similar results were obtained for the $x$ = 0.15 ones. The peaks corresponding to the OP phase appear after 2 h. After 7 h, the peaks corresponding to the initial mixture are not more visible and the OP phase seems to be the predominant one. This situation is maintained up 24 h of milling. The behavior is similar to that reported by Moure et al. [23], confirming that orthorhombic perovskite phases can be obtained by mechanosynthesis, for both Ni and Co-doped $ErMnO_3$ oxides despite the different oxidation states and electronic behaviors. As it was reported in [23], during the milling process, the impact of the balls on the mixture and the shear effect on the pot walls generate pressures that can be on the order of GPa [24] similar to that necessary to occur HS → OP transformation. The mechanical energy supplied helps the material with the highly distorted perovskite structure to be stabilized, similarly to the external pressure used in the method described in [21,22]. Moreover, the milled powder has a high average crystalline strain which has a hydrostatic like component, because of the disorder and defects introduced by the impacts. It facilitates the synthesis of OP structure materials with a high degree of distortion [25], as that imposed by Jahn–Teller effect in $ErMnO_3$ based materials.

To study the temperature range where the OP polymorph exists before its transformation to the HS form, the mechanosynthesized powders were thermally treated at different temperatures. Fig. 2 shows the results for the compositions with Ni and Co fixed at $x$ = 0.05. For both solid solutions the

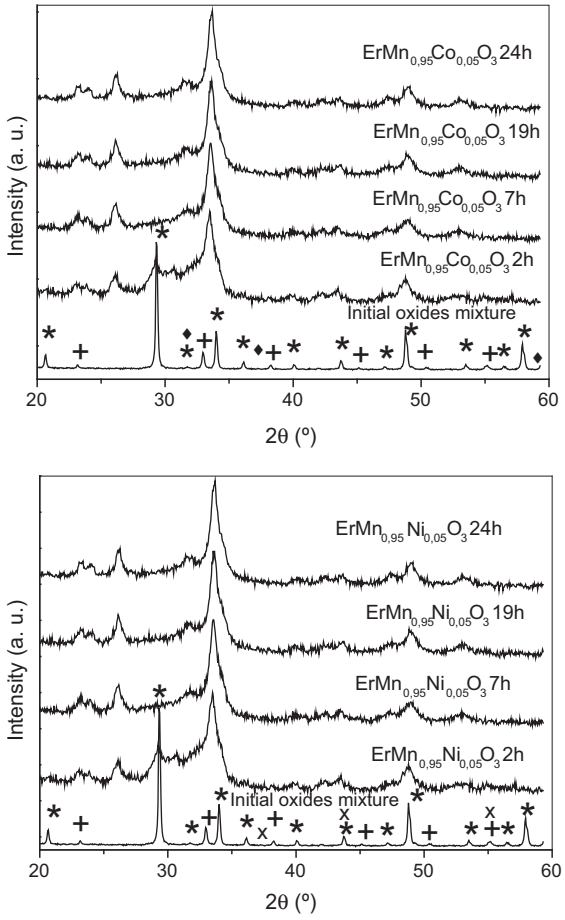


Fig. 1. XRD patterns of the stoichiometric mixture of $Er_2O_3$, $Mn_2O_3$, NiO, $Co_3O_4$ precursor of $ErMn_{0.95}Ni_{0.05}O_3$ and $ErMn_{0.95}Co_{0.05}O_3$, after different milling times. (Initial oxides—*: $Er_2O_3$; +: $Mn_2O_3$; x: NiO; ◆: $Co_3O_4$).

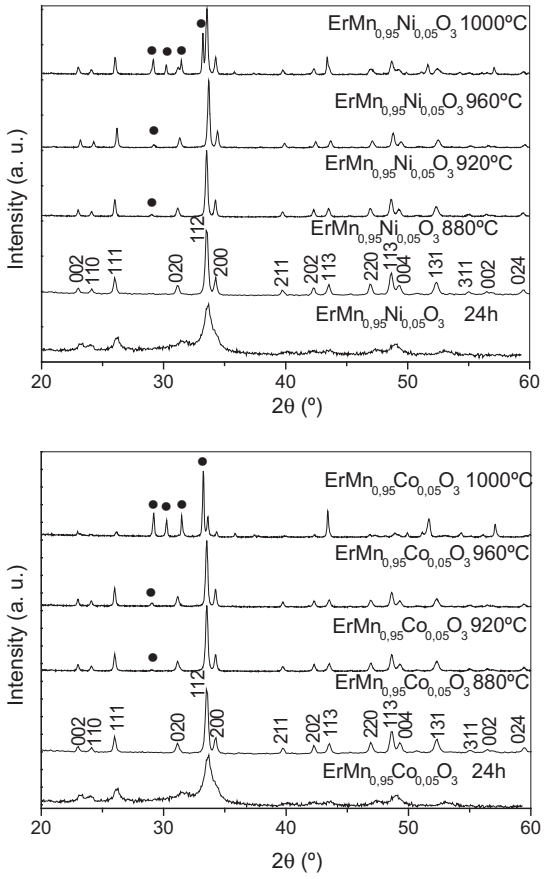


Fig. 2. XRD patterns after several thermal treatments of $ErMn_{0.95}Ni_{0.05}O_3$ and $ErMn_{0.95}Co_{0.05}O_3$ mechanosynthesized phase (•: peaks corresponding to the HS phase). Powder ceramics precursors after 24 of milling without thermal treatment are shown for comparison.

perovskite polymorph results in a well crystallized powder at 880 °C, while traces of the HS phase are observed from 920 °C.

Similar results to those reported for $ErMn_{1-x}Ni_xO_3$ solid solution [23] also confirmed in this work, are observed for $ErMn_{1-x}Co_xO_3$ system. In fact, Fig. 2 reports the stabilization of the OP-type phase for $ErMn_{0.95}Co_{0.05}O_3$ composition, which remains as a single phase up to 920–960 °C, when traces of the HS polymorph can also be detected. This means that mechanochemical process changes the conditions at which perovskite structure can be obtained as single phase for Co-doped compounds. In Ref. [26], it was shown that at least $x = 0.3$ values were necessary to obtain a single OP phase for this $ErMn_{1-x}Co_xO_3$ solid solution, if a classical solid state synthesis route is employed, with heating at 1000 °C followed by sintering at temperatures up to 1425 °C. Mechanosynthesis was shown as an alternative to the high pressure methods to achieve highly distorted $ErMnO_3$ orthorhombic perovskite phase, due to the high energy applied during the prolonged milling [23]. The same mechanism occurs with the addition of a small amount of Co to the initial mixture. The reduction of the particle size to the nanometer scale, around 20–30 nm, and the energy supplied allow an intimate mixture during milling, favoring the Co incorporation to the highly distorted perovskite structure.

The stabilization of the perovskite structure is different for Ni or Co doped phases. This fact is clearly observed as the temperature of the thermal annealing increases (Fig. 2). The reflection peaks corresponding to the HS phase begin to appear at 920 °C, becoming the predominant phase at 1000 °C for the Co-doped compound, while the OP polymorph remains as the main phase for the Ni-doped material at the same temperature. That is to say, the OP phase is more stable for the $ErMn_{0.95}Ni_{0.05}O_3$ than for the $ErMn_{0.95}Co_{0.05}O_3$ composition. This fact can be related to the variable valence state of the cobalt cations ($Co^{2+}$ or $Co^{3+}$), while $Ni^{2+}$ is much more stable. When divalent cations are incorporated to the structure, the Jahn–Teller $Mn^{3+}$ cation transforms to $Mn^{4+}$, which is not a Jahn–Teller cation. For Co doping, it has been previously reported [20,26] that the presence of $Co^{3+}$ prevents the formation of $Mn^{4+}$, so the cooperative Jahn–Teller effect imposes a high distortion of the perovskite structure, in such a way that the HS structure is energetically favorable, giving rise to the phase transition. For the Ni doping, the high stability of $Ni^{2+}$ state makes that each Ni cation induces a +4 valence state for Mn cation, being the perovskite structure more stable. In any case, the addition of lower amounts of Co stabilizes the perovskite structure with respect to $ErMnO_3$, otherwise the

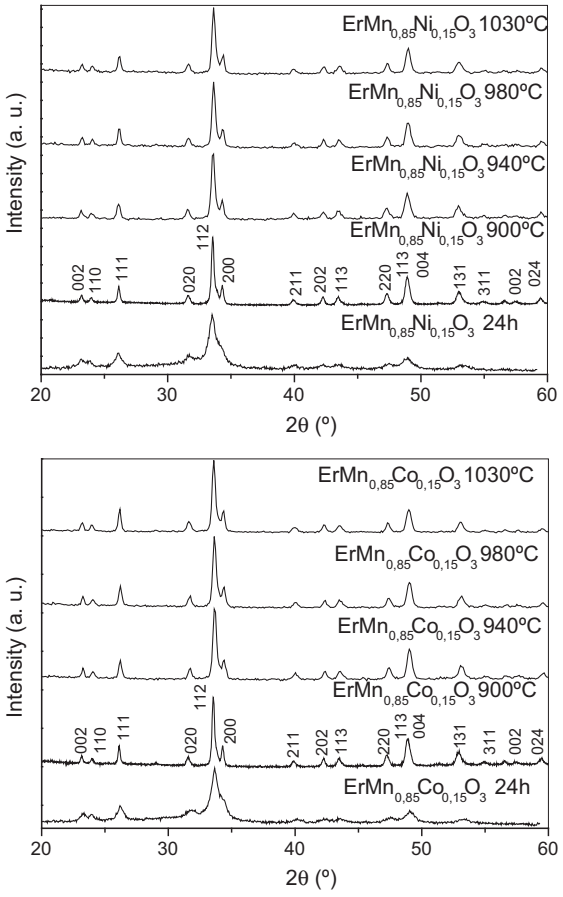


Fig. 3. XRD patterns after several thermal treatments of $ErMn_{0.85}Ni_{0.15}O_3$ and $ErMn_{0.85}Co_{0.15}O_3$ mechanosynthesized phases. Powder ceramics precursors after 24 of milling without thermal treatment are shown for comparison.

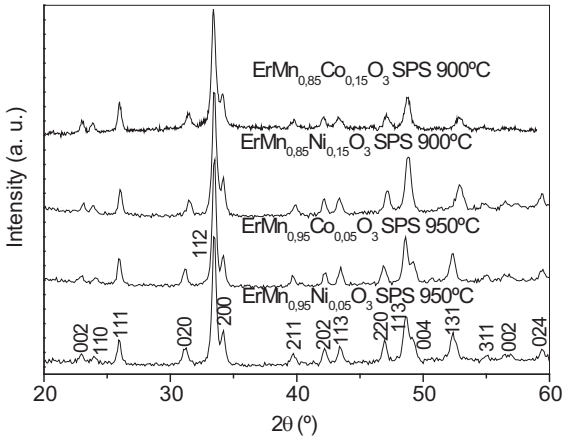


Fig. 4. XRD patterns of SPS ceramics of $ErMn_{1-x}Ni_xO_3$ and $ErMn_{1-x}Co_xO_3$ ($x = 0.05$, 0.15) processed at 900 or 950 °C for 1 min.

structure is totally transformed to hexagonal at 1000 °C. For the $ErMn_{0.95}Co_{0.05}O_3$ composition there is a mixture at such temperature.

The increase of the stability of the perovskite structure with Ni and Co doping is more clearly observed for the $x = 0.15$ compositions. Fig. 3 shows the X-ray diffraction patterns after thermal treatment of $ErMn_{0.85}Ni_{0.15}O_3$ and $ErMn_{0.85}Co_{0.15}O_3$ mechanosynthesized phases. It is observed that even at 1030 °C, the orthorhombic perovskite appears free of traces of the hexagonal structure. That is, the higher the $x$ values for both Ni and Co, the higher the stabilization temperatures range of the perovskite structure. It also confirms that with the use of mechanosynthesis, the perovskite structure can be stabilized at lower amounts of Ni and Co than that needed when the solid solutions are processed by solid state reaction ($x = 0.2$ and 0.3) respectively [20].

Due to the problems for stabilizing the OP phase at increasing temperatures, Spark Plasma Sintering (SPS) was successfully used to process relatively dense $ErMnO_3$ ceramics with perovskite structure. This technique was also used for $ErMn_{1-x}Ni_xO_3$ and $ErMn_{1-x}Co_xO_3$ powders. The results are shown in Fig. 4. Pure OP phases are observed for both Ni and Co doping cations, indicating that the pressure and low temperatures used during the SPS process help to maintain the structure in well formed ceramics.

The low temperature employed during the SPS process gives place to nanostructured ceramics, as it was previously observed in $ErMnO_3$ ceramics [23], and with densities higher than 90% in all cases. To illustrate this, Fig. 5 shows the TEM studies for the $ErMn_{0.85}Co_{0.15}O_3$ ceramics processed by SPS at 900 °C. Grains are in the nanometric scale, with an average mean size of 39 nm measured in a population of 150 grains, approximately. The largest measured grains have sizes of 80 nm (Fig. 5b). The detail of one grain, also shown in Fig. 5c, shows the good crystallinity achieved during the SPS process despite the low temperature used. The interplanar distance shown in Fig. 5c (3.4 Å) fits well with that corresponding to (1 1 1) plane family of the orthorhombic perovskite structure.

Fig. 6a shows the ZFC/FC cycles carried out on the $ErMn_xNi_{1-x}O_3$ and $ErMn_xCo_{1-x}O_3$ ceramics processed at 900 °C. The insets represent the dependence of the inverse of the magnetic susceptibility as a function of temperature, in the paramagnetic region. From these data, the values of $\mu_{eff}$ and Curie–Weiss temperature ($\Theta$) are obtained. Typical behaviors of antiferromagnetic interactions are observed for both Ni ($\Theta = -18$ K and $-10$ K for $x = 0.05$ and 0.15, respectively) and Co doping ($\Theta = -17$ K and $-11$ K for $x = 0.05$ and 0.15, respectively).

The results of the substitutions of Ni for Mn correlate well with those found in our previous works [23,26], in which values of $\Theta = -14$ K and $-6$ K for $x$(Ni) = 0.10 and 0.20, respectively, were reported. Thus the incorporation of $Ni^{2+}$ to the lattice of $ErMnO_3$ leads to a progressive increase of the ferromagnetic behavior, which is well established for $x = 0.33$ and above [26]. This increase is less pronounced for the Co incorporation. The value measured at $x$(Co) = 0.15 does not differ from the value reported for $x$(Co) = 0.20 [26] ($\Theta = -11$ K for both compositions), indicating that $Co^{3+}$ could be present in an important ratio with regard to $Co^{2+}$.

The values of the effective moment $\mu_{eff}$ are also obtained from the insets graphs. First of all, it should be recalled that an important contribution comes from the $Er^{3+}$ free-ion, whose

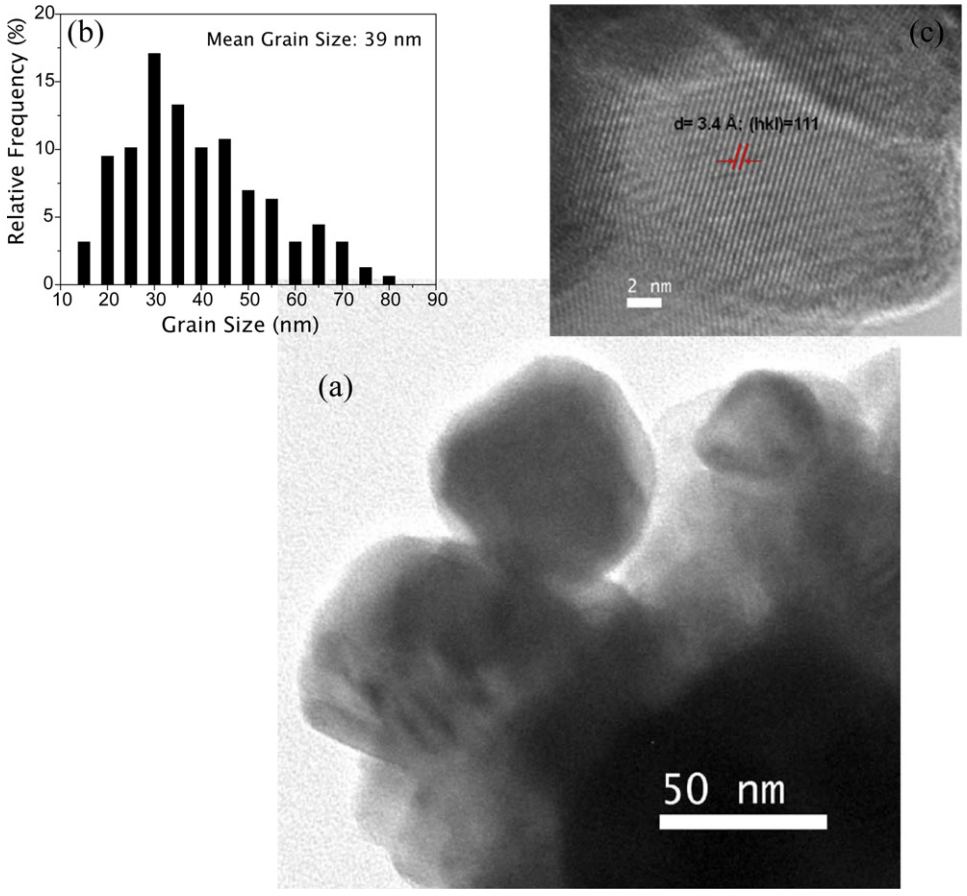


Fig. 5. (a) TEM images of grains corresponding to $ErMn_{0.85}Co_{0.15}O_3$ ceramic processed by SPS at 900 °C; (b) the corresponding grain size distribution; and (c) high resolution image corresponding to the (1 1 1) planes of the OP structure.

magnetic moment is $9.58\mu_B$, leaving then a magnetic contribution of the Mn + *Me* sublattice (*Me* = Ni, Co) which is compatible with the expected magnetic moment of the transition metals *Me* [26]. The overall effective moments are similar for $x = 0.05$ doping contents ($\mu_{eff} = 10.52\mu_B$ for Ni and $10.46\mu_B$ for Co, respectively), but are higher for Co doping at $x = 0.15$ ($\mu_{eff} = 10.41\mu_B$ for Ni and $10.53\mu_B$ for Co, respectively), in a similar trend to that observed in Ref. [26]. This difference can be easily explained considering the fact that $Co^{2+}$ ions ($S = 3/2$) have higher magnetic moments than $Ni^{2+}$ ions ($S = 1$), but we cannot exclude the presence of $Co^{3+}$ with a high-spin state ($S = 2$; $4.90\mu_B$). This behavior is in good agreement with our observations in Fig. 2, where the stability of the Co-doped OP was found to be lower than that of the Ni-doped materials. It was related to the presence of $Co^{3+}$ that diminishes the transformation from $Mn^{3+}$ to $Mn^{4+}$. The difference in $\mu_{eff}$ between both compositions is lower at small doping amounts, because it is then governed by Mn contributions.

The ZFC/FC curves present a reversible behavior in the paramagnetic regime, above a reversible temperature $T = T_{rev}$, decreasing as the doping content increases (from $T_{rev}$ = 32–33 K for $x = 0.05$ to 21–22 K for $x = 0.15$). Similar trend was reported in Ref. [26] for $x$(Ni) = 0.20 ($T_{rev}$ = 18 K) and attributed to the presence of small amounts of diluted $Mn^{4+}$, and not to ferromagnetic interactions between Mn and the doping cation Ni, which are absent for $x = 0$, and quite diluted in samples with $x = 0.05$–$0.20$. At higher doping concentrations, strong ferromagnetic interactions develop and the system becomes a typical example of canting antiferromagnetism ($x = 0.33$; $T_c = 40$ K) before becoming a full ferromagnet ($x = 0.40$; $T_c = 62$ K) (see Fig. 6 in Ref. [26]). In the case of diluted magnetic systems, as those studied in this work, the behavior is the same for both Ni and Co doped materials, ruling out the influence of those interactions with Mn.

Magnetization loops are shown in Fig. 6b. The curves at low doping content ($x = 0.05$) resemble those observed for non-doped and slightly doped materials, that is, negligible coercive fields (see inserts in Fig. 6b) [23]. The magnetization slightly increases for $x = 0.15$ compared to $x = 0.05$, since the main contribution comes from the $Mn^{3+}$–$Mn^{4+}$ interaction. The increase in the dopant amounts increases the appearance of $Mn^{4+}$ cations, thus increasing the interaction. Again, these contributions are somewhat hidden by the large magnetic moment of the $Er^{3+}$ ions which, at saturation, should be of the order of $9\mu_B$ for a free ion, in the absence of any crystal field splitting.

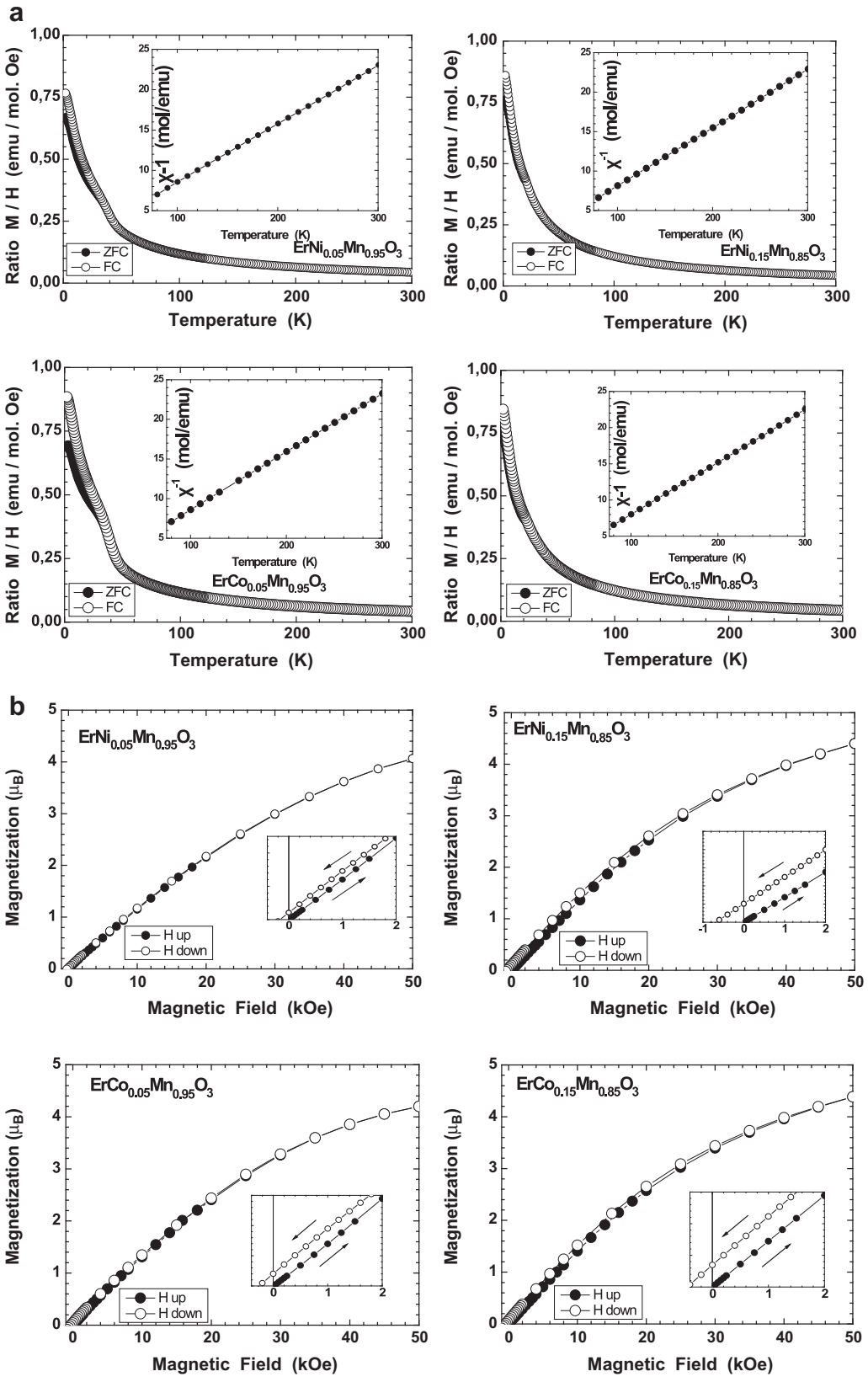


Fig. 6. (a) Field cooling (FC) and zero field cooling (ZFC), main panels and inverse of the susceptibility (inserts); (b) magnetisation cycles at 2 K of $ErMn_{1-x}Ni_xO_3$ and $ErMn_{1-x}Co_xO_3$ ($x = 0.05, 0.15$) ceramics treated at 900 °C.

## 4. Conclusions

Single-phase orthorhombic perovskites belonging to $ErMn_{1-x}Ni_xO_3$ and $ErMn_{1-x}Co_xO_3$ solid solutions ($x = 0.05$ and 0.15) were obtained by mechanosynthesis for the first time. The prolonged and high energetic milling allows a distorted structure to be stabilized with lower doping amounts than those needed in classical solid state processes.

The temperature range of stability for the perovskite structure depends on the nature of the doping cation. The high stability of $Ni^{2+}$ allows the $Mn^{3+}$ cations to be oxidized to $Mn^{4+}$, decreasing the cooperative Jahn–Teller effect, and thus the OP instability, increasing in this way the range of temperatures where such phase exists. On the contrary, the twofold valence state of Co ($Co^{2+}$ and $Co^{3+}$) does not change so large amounts of $Mn^{3+}$ cations on the $ErMn_{1-x}Co_xO_3$ compositions, reducing the stability of the perovskite structure. By increasing the doping amount to $x = 0.15$, single phase perovskite structures were observed even at 1030 °C.

Spark Plasma Sintering was used to obtain dense ceramics, keeping the OP structure at low temperatures (900–950 °C), maintaining the grain size at the nanoscale range. Magnetic behavior correlates to that previously reported in the solid solutions with $ErNi_xMn_{1-x}O_3$ and $ErCo_xMn_{1-x}O_3$ compositions ($x \geq 0.20$), obtained by conventional solid-state synthesis. It is then proved the effectiveness of the mechanosynthesis as a simpler route to isolate orthorhombic-perovskites manganites of rare earths with small radius, instead of the usual methods using high pressures in the order of GPa.

## Acknowledgments

This work was supported by Spain PROFIT CIT-120000-2007-50 and MICINN MAT2008-06785-C02-02-E. Drs A. Castro and T. Hungría acknowledge the financial support of the Spanish MICINN (project MAT2010-18543). Drs. A. Moure and T. Hungría are indebted to the CSIC (MICINN) of Spain for the ''Junta de Ampliación de Estudios'' contracts (Refs JAEDOC087 and JAEDOC082, respectively). The authors thank the assistance of the PFN2, Toulouse (France), where the SPS experiments were performed in the frame of the Action FR2009-0093 (Spanish MICINN).

## References

[1] A.P. Ramirez, Colossal magnetoresistance, J. Phys. Condens. Matter 9 (1997) 8171–8199.
[2] T. Kimura, T. Goto, H. Shintani, K. Ishizaka, T. Arima, Y. Tokura, Magnetic control of ferroelectric polarization, Nature 426 (2003) 55–58.
[3] B. Lorenz, Y.Q. Wang, C.W. Chu, Ferroelectricity in perovskite $HoMnO_3$ and $YMnO_3$, Phys. Rev. B 76 (2007) 104405-1–104405-5.
[4] C.Y. Ren, Atomic, electronic, and ferroelectric properties of manganite $RMnO_3$ (R = Ho, Er, Tm, Lu) in hexagonal and orthorhombic phases, Phys. Rev. B 79 (2009) 125113-1–125113-10.
[5] O. Muller, R. Roy, The Major Ternary Structural Families, Springer-Verlag, NY, 1974, p. 357.
[6] R.D. Shannon, Revised effective ionic-radii and systematic studies of interatomic distances in halides and chalcogenides, Acta Cryst. A 32 (1976) 751–767.
[7] J.B. Goodenough, Theory of the role of covalence in the perovskite-type manganites [La, M(II)]$MnO_3$, Phys. Rev. 100 (1955) 564–573.
[8] E.O. Wollan, W.C. Koehler, Neutron diffraction study of the magnetic properties of the series of perovskite-type compounds [$(1-x)$La, $x$Ca]$MnO_3$, Phys. Rev. 100 (1955) 545–563.
[9] E. Pollert, S. Krupicka, E. Kiuzmikova, Structural study of $Pr_{1-x}Ca_xMnO_3$ and $Y_{1-x}Ca_xMnO_3$ perovskites, J. Phys. Chem. Solids 43 (1982) 1137–1145.
[10] O. Peña, A.B. Antunes, G. Martínez, V. Gil, C. Moure, Inter-network magnetic interactions in $GdMe_xMn_{1-x}O_3$ perovskites (Me = transition metal), J. Magn. Magn. Mater. 310 (2007) 159–168.
[11] F. Ye, B. Lorenz, Q. Huang, Y.Q. Wang, Y.Y. Sun, C.W. Chu, J.A. Fernandez-Baca, P. Dai, H.A. Mook, Incommensurate magnetic structure in the orthorhombic perovskite $ErMnO_3$, Phys. Rev. B 76 (2007) 060402-1–060402-4.
[12] Y.H. Huang, H. Fjellvg, M. Karppinen, B.C. Hauback, H. Yamauchi, J.B. Goodenough, Crystal and magnetic structure of the orthorhombic perovskite $YbMnO_3$, Chem. Mater. 18 (2006) 2130–2134.
[13] C. Moure, M. Villegas, J.F. Fernández, J. Tartaj, P. Durán, Phase transition and electrical conductivity in the system $YMnO_3$–$CaMnO_3$, J. Mater. Sci. 34 (1999) 2565–2568.
[14] M.N. Iliev, B. Lorenz, A.P. Litvinchuk, Y.Q. Wang, Y.Y. Sun, C.W. Chu, Structural, transport, magnetic properties and Raman spectroscopy of orthorhombic $Y_{1-x}Ca_xMnO_3$ ($0 \leq x \leq 0.5$), J. Phys. Condens. Matter 17 (2005) 3333–3341.
[15] D. Vega, G. Polla, A.G. Leyva, P. Konig, H. Lanza, A. Esteban, H. Aliaga, M.T. Causa, M. Tovar, B. Alascio, Structural phase diagram of $Ca_{1-x}Y_xMnO_3$: characterization of phases, J. Solid State Chem. 156 (2001) 458–463.
[16] A.B. Antunes, O. Pena, C. Moure, V. Gil, G. Andre, Structural and magnetic properties of Er(Co, Mn)$O_3$ perovskite, J. Magn. Magn. Mater. 316 (2007) 652–655.
[17] P.M. Woodward, T. Vogt, D.E. Cox, A. Arulraj, C.N.R. Rao, P. Karen, A.K. Cheetham, Influence of cation size on the structural features of $Ln_{1/2}A_{1/2}MnO_3$ perovskites at room temperature, Chem. Mater. 10 (1998) 3652–3665.
[18] N. Sdiri, M. Bejar, E. Dhahri, The effect of the B-site size on the structural, magnetic and electrical properties of $La_{0.7}Ca_{0.3}MnO_{3-\delta}$ compounds, J. Magn. Magn. Mater. 311 (2007) 512–516.
[19] O. Peña, M. Bahout, D. Gutierrez, P. Duran, C. Moure, Interacting networks and spin polarization in (Dy, Ca)$MnO_3$, Solid State Sci. 5 (2003) 1217–1227.
[20] C. Moure, D. Gutierrez, O. Peña, P. Duran, Structural characterization of $YMe_xMn_{1-x}O_3$ (Me = Cu, Ni, Co) perovskites, J. Solid. State Chem. 163 (2002) 377–384.
[21] J.S. Zhou, J.B. Goodenough, J.M. Gallardo-Amores, E. Moran, M.A. Alario-Franco, R. Caudillo, Hexagonal versus perovskite phase of manganite $RMnO_3$ (R = Y, Ho, Er, Tm, Yb, Lu), Phys. Rev. B 74 (2006) 014422-1–014422-7.
[22] B. Lorenz, Y.Q. Wang, Y.Y. Sun, C.W. Chu, Large magnetodielectric effects in orthorhombic $HoMnO_3$ and $YMnO_3$, Phys. Rev. B 70 (2004) 212412-1–212412-4.
[23] A. Moure, T. Hungria, A. Castro, J. Galy, O. Peña, J. Tartaj, C. Moure, Mechanosynthesis of the orthorhombic perovskites $ErMn_{1-x}Ni_xO_3$ ($x = 0$, 0.1). Processing and characterization of nanostructured ceramics, Chem. Mater. 22 (2010) 2908–2915.
[24] C. Suryanarayana, Mechanical alloying and milling, Prog. Mater. Sci. 46 (2001) 1–184.
[25] M. Alguero, J. Ricote, T. Hungria, A. Castro, High-sensitivity piezoelectric, low-tolerance-factor perovskites by mechanosynthesis, Chem. Mater. 19 (2007) 4982–4990.
[26] O. Peña, A.B. Antunes, M.N. Baibich, P.N. Lisboa-Filho, V. Gil, C. Moure, Spin reversal and magnetization jumps in $ErMe_xMn_{1-x}O_3$ perovskites (Me = Ni Co), J. Magn. Magn. Mater. 312 (2007) 78–90.